1

Introduction to Organocatalytic Cycloaddition Reaction

Yin Wei[1] *and Min Shi*[1,2]

[1] *Chinese Academy of Sciences, University of Chinese Academy of Sciences, Center for Excellence in Molecular Synthesis, Shanghai Institute of Organic Chemistry, State Key Laboratory of Organometallic Chemistry, 345 Lingling Road, Shanghai 200032, China*
[2] *East China University of Science and Technology, Institute of Fine Chemicals, School of Chemistry and Molecular Engineering, Key Laboratory for Advanced Materials, 130 Mei Long Road, Shanghai 200237, China*

COPYRIGHTED MATERIAL

1.1 General Introduction

Carbo- and heterocycles as core structures exist in a variety of pharmacological agents and natural products [1]. Therefore, development of novel and efficient methods to synthesize carbo- and heterocyclic compounds is a topic of paramount importance in modern organic synthesis. Although a variety of highly efficient methodologies for the synthesis of various carbo- and heterocyclic systems exist, the development of novel strategies involving readily accessible starting materials, reduced numbers of transformation steps and purification procedures, and high selectivities (chemo-, regio-, and stereoselectivity) is in continuous demand. Among the synthetic methods to access carbo- and heterocyclic compounds, cycloaddition reactions catalyzed by utilizing nucleophilic organocatalysts, such as tertiary amines, phosphines, or *N*-heterocyclic carbenes (NHCs) represent one of the most commonly used and efficient methods. In general, organocatalytic cycloaddition reactions can be processed based on a zwitterion-oriented synthetic strategy depicted in Scheme 1.1 in which the addition of a nucleophilic organocatalyst to the electrophilic substrate generates the zwitterion intermediate, which then undergoes the addition with the second electrophilic substrate followed by cyclization and releasing the catalyst to give carbo- and heterocyclic products. Taking advantage of the zwitterion-oriented synthetic strategy, subtle tuning catalysts, substrates, and the reaction conditions can provide divergent synthetic routes to access different carbo- and heterocyclic compounds. Thus, this research field has attracted a lot of attention in recent decades. Many research groups such as Lu's group [2], Kwon's group [3], Shi's group [4], Zhang's group [5], Guo's group [6], Huang's group [7], Tong's group [8], and so on have contributed a series of research works on organocatalytic

Organocatalytic Cycloadditions for Synthesis of Carbo- and Heterocycles, First Edition.
Min Shi, Yin Wei, Mei-Xin Zhao, and Jun Zhang.
© 2018 Wiley-VCH Verlag GmbH & Co. KGaA. Published 2018 by Wiley-VCH Verlag GmbH & Co. KGaA.

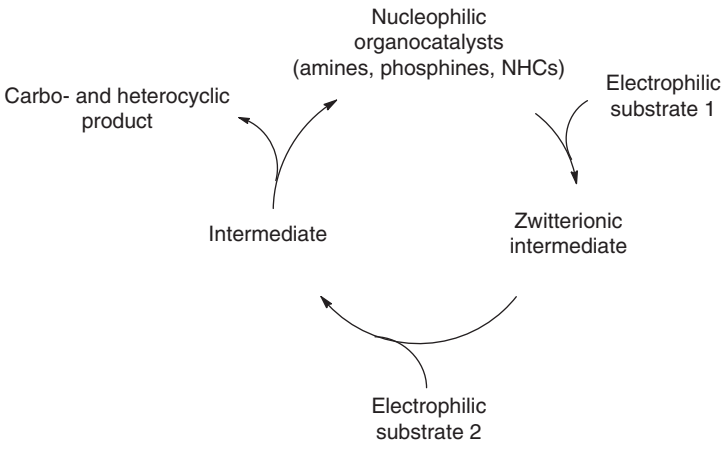

Scheme 1.1 General mechanism of organocatalytic cycloaddition reaction.

cycloaddition reactions, which have enriched the literature on the synthetic methods to access carbo- and heterocyclic compounds.

Although several reviews [9] have discussed the progresses of organoamine-catalyzed, organophosphine-catalyzed, and NHC-promoted cycloaddition reactions, comprehensive literature fully covering these topics is lacking. We would like to concentrate our discussion and assessment on the following issues: (i) in-depth investigations of reaction mechanisms for zwitterion-oriented cycloadditions promoted by organoamines and organophosphines as well as NHCs; (ii) synthesis of different products from the same starting material(s) by subtle choice of different catalysts; (iii) how to control the chemo-, regio-, and stereoselectivity; and (iv) synthetic applications of these organocatalytic cycloaddition reactions. We hope that this book will satisfy the expectations of experienced researchers and graduated students who are interested in the development of the field and are looking for complete and up-to-date information on the chemistry of organocatalytic cycloaddition reactions.

1.2 General Mechanistic Insights into Cycloadditions Catalyzed by Nucleophilic Organocatalysts

Most of organocatalytic cycloaddition reactions are initiated by the conjugate addition of a nucleophilic catalyst to the electrophilic substrate producing a zwitterionic intermediate, which can then go through various cycloaddition pathways depending on the substrates, nature of catalyst, and the reaction conditions. The selected examples were depicted to demonstrate the mechanisms for common organocatalytic cycloaddition reactions.

1.2.1 Mechanisms for Common Organoamine-catalyzed Cycloaddition Reactions

In the early 1980s, Wynberg and Staring began a systematic investigation of the formal [2+2] cycloaddition between ketenes and aldehydes [10]. The reaction

mechanism was proposed to proceed through the attack of the chiral amine catalyst **1** or **2** on the ketene **3**, which leads to the formation of a highly reactive amidonium enolate **4** (Scheme 1.2). This enolate then adds to an electrophilic aldehyde to generate an alkoxide that can close onto the acylammonium ion **5**, subsequently releasing the chiral amine catalyst and forming the [2+2] cycloadduct β-lactone **6**. In a classic series of studies, it was shown that both enantiomers of the product could be obtained simply through judicious choice of the alkaloid catalyst. Subsequent analysis of the crystal and solution structures of these compounds provides a clear rationale for the factors influencing the stereoselectivity [11]. In the context of organoamine-catalyzed reactions, it is interesting to note that enhanced nucleophilicity at C2 played a role in the formation of the carbon–carbon bond while enhanced electrophilicity at C1 played a role in the final cyclization step.

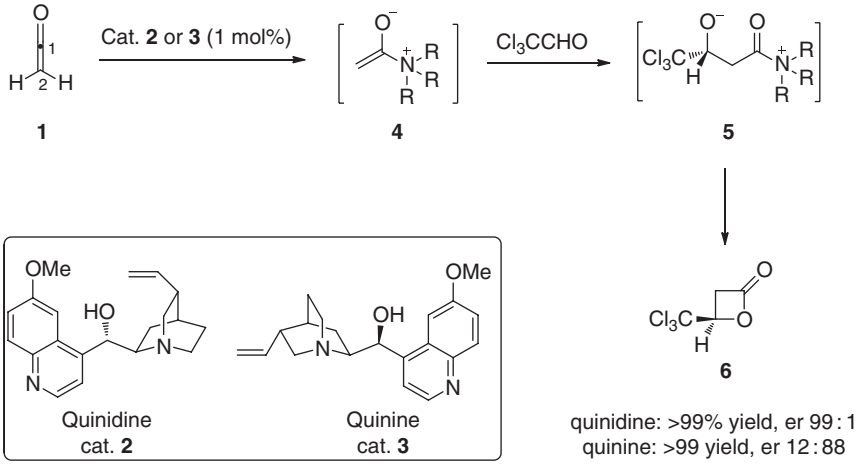

Scheme 1.2 The proposed mechanism for the formal [2+2] cycloaddition between ketenes and aldehydes.

Shi and co-workers reported that utilizing DABCO as the catalyst, *N*-tosylimines **7** underwent formal [2+2] cycloadditions with 2,3-butadienoates to afford azetidine derivatives **8**; however, switching the catalyst to DMAP, the formal [4+2] cycloaddition occurred to give dihydropyridine derivatives **9** [12] (Scheme 1.3). The nuclophilicities of organoamines probably affected the reaction pathways. They proposed the plausible mechanisms as shown in Scheme 1.4. The nitrogen Lewis bases (LB) DABCO and DMAP act as a nucleophilic organocatalyst and produce the key intermediate **10**, which exists as a resonance-stabilized zwitterionic intermediate **10** (enolate) or **11** (allylic carbanion). In the case of DABCO, the allylic carbanion **11** adds to the *N*-tosylated imine to give the intermediate **12**, which undergoes an intramolecular nucleophilic attack (Michael type) to give another zwitterionic intermediate **13**. The elimination of NR_3 from **13** affords product **8** and regenerates DABCO (Scheme 1.4a). However, in the case of DMAP, the enolate **10** adds to the *N*-tosylated imine to afford the intermediate **14**, which adds to another *N*-tosylated imine to give the intermediate **15**. The proton transfer

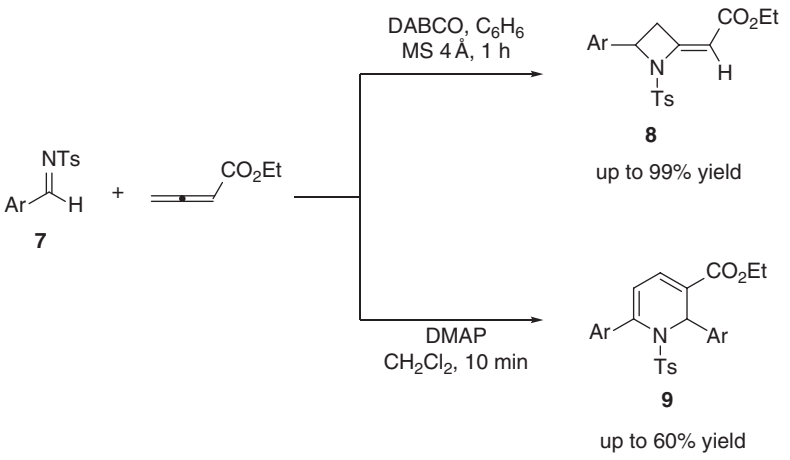

Scheme 1.3 The formal [2+2] cycloaddition versus [4+2] cycloaddition catalyzed by amines.

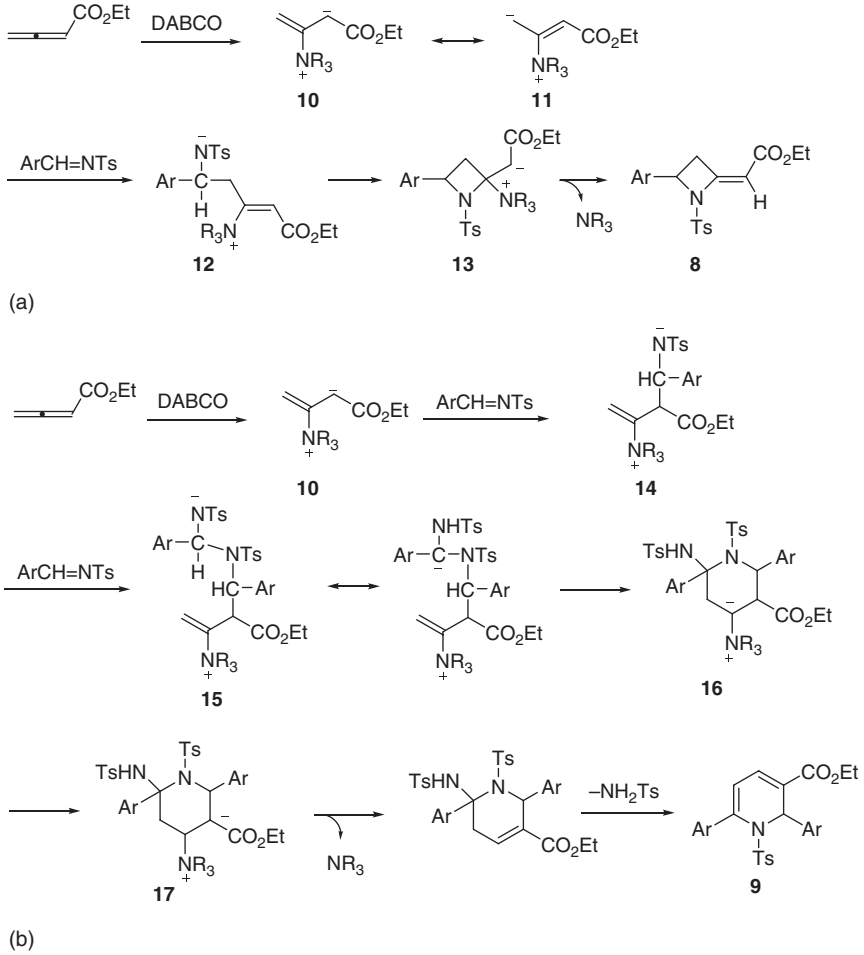

Scheme 1.4 Proposed mechanisms for the formal [2+2] cycloaddition versus [4+2] cycloaddition catalyzed by amines.

produces the intermediate **16**, and the subsequent intramolecular Michael addition gives the intermediate **17**. Proton shift and NHTs elimination furnish product **9** and regenerate DMAP.

Shi's group reported another chemoselective [4+2] versus [2+2] cycloaddition between allenoates and dithioesters **18**, which can be controlled by switching the nucleophilic amine catalyst to give [4+2] product **19** and [2+2] cycloaddition product **20** [13] (Scheme 1.5). A plausible mechanism is depicted in Scheme 1.6 to account for the selective control. The [4+2] and [2+2] cycloaddition reactions are initiated by the formation of zwitterionic intermediate **21** via the nucleophilic addition of amine to allenoate. When amine is DABCO, the thiophilic attack of **21** on the sulfur atom of the thiocarbonyl group in **18** generates intermediate **22**. The subsequent cyclization delivers an intermediate **23**, which eliminates the catalyst to afford product **19**. Based on this mechanism, the reaction of dithioesters bearing electron-deficient R^2 group with allenoate is favored because the negative charge in intermediate **22** can be stabilized by delocalization. This is probably why they have better chemoselectivity. When the amine catalyst is **26** or β-isocupreidine (β-ICD), the nucleophilic attack of zwitterionic intermediate **21** on the carbon atom of the thiocarbonyl group in **18** is preferred to give an intermediate **24**, perhaps due to the observation that the hydrogen-bonding interaction between the catalyst with its hydrogen-bonding donor and the substrate leads to the chemoselective [2+2] exceeding over [4+2] cycloaddition (Scheme 1.6). Thus, the C–S bond is formed to generate an intermediate **25** and then the catalyst is released to give product **20**.

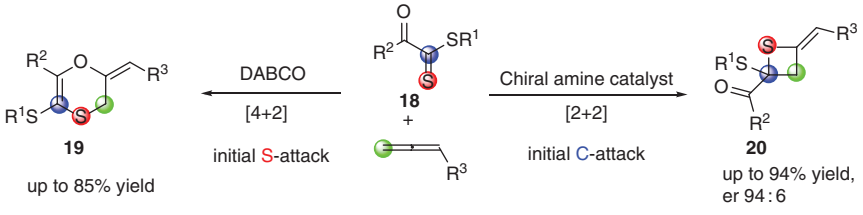

Scheme 1.5 [4+2] versus [2+2] cycloaddition between allenoates and dithioesters.

Although the mechanisms for common organoamino-catalyzed cycloaddition reactions are proposed from time to time, the detailed mechanistic studies are still scarcely reported. Li and Du [14] investigated the mechanism of the DMAP-catalyzed [2+4] cycloaddition between γ-methylallenoate and phenyl(phenyldiazenyl) methanone by using density functional theory (DFT) calculations for a better understanding of the mechanistic details. They investigated two possible reaction pathways as shown in Scheme 1.7. Mechanism A includes four reaction steps: (i) the nucleophilic attack of catalyst DMAP on **27** forms the zwitterionic adduct **28**, (ii) the γ-addition of **28** to **29** generates an intermediate γ-**30**, (iii) the intermediate γ-**30** undergoes an intramolecular Michael addition to afford an intermediate γ-**31**, and (iv) the catalyst elimination from γ-**31** yields the final product γ-**32**. Mechanism B comprises three steps: (i) the nucleophilic addition of catalyst DMAP to **27** generates a zwitterionic intermediate **28**, which is the same as that in mechanism A,

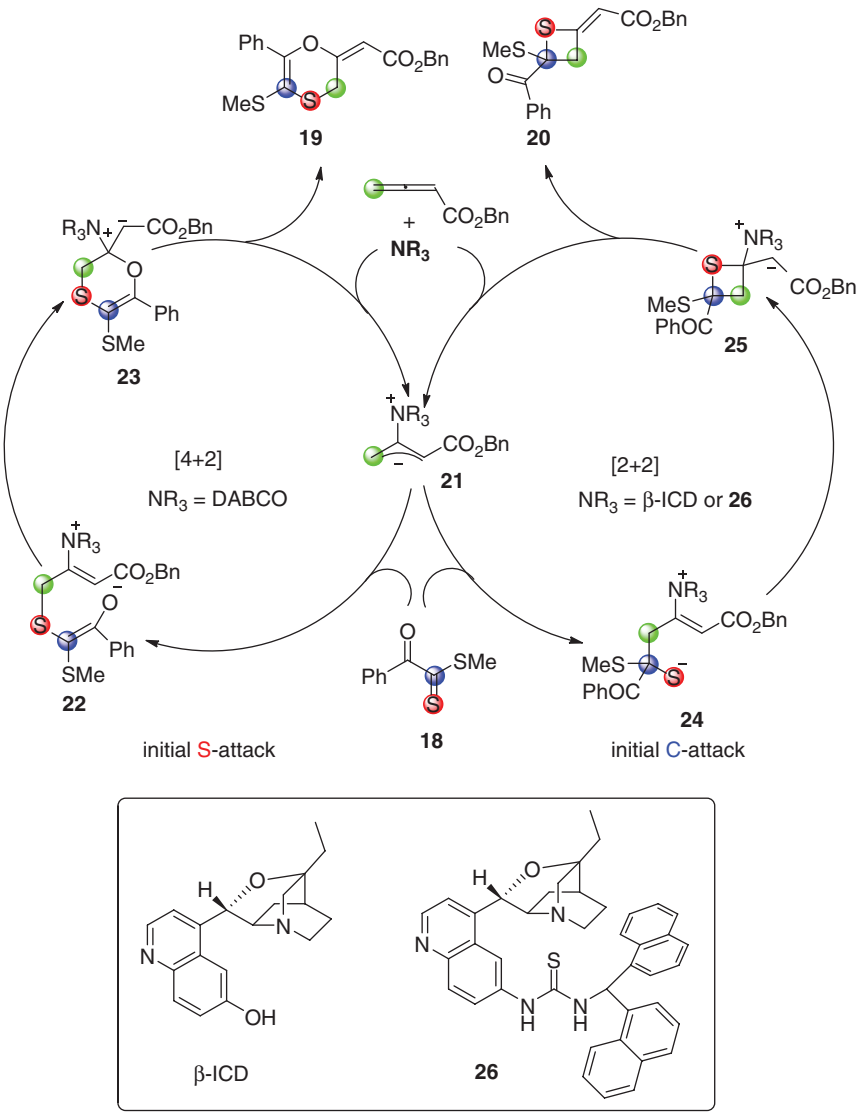

Scheme 1.6 [4+2] versus [2+2] cycloaddition between allenoates and dithioesters.

(ii) α-addition of **28** to **29** affords an intermediate α-**33**, and (iii) the intermediate α-**33** is transformed to the final product α-**34** via a concerted intramolecular cyclization and catalyst elimination process. Through a series of DFT calculations, the calculated results support the proposed mechanism A. In the DMAP-catalyzed [2+4] cycloaddition between γ-methyl allenoate and phenyl(phenyldiazenyl)methanone, catalytic cycle can be characterized by four steps: (i) nucleophilic attack of

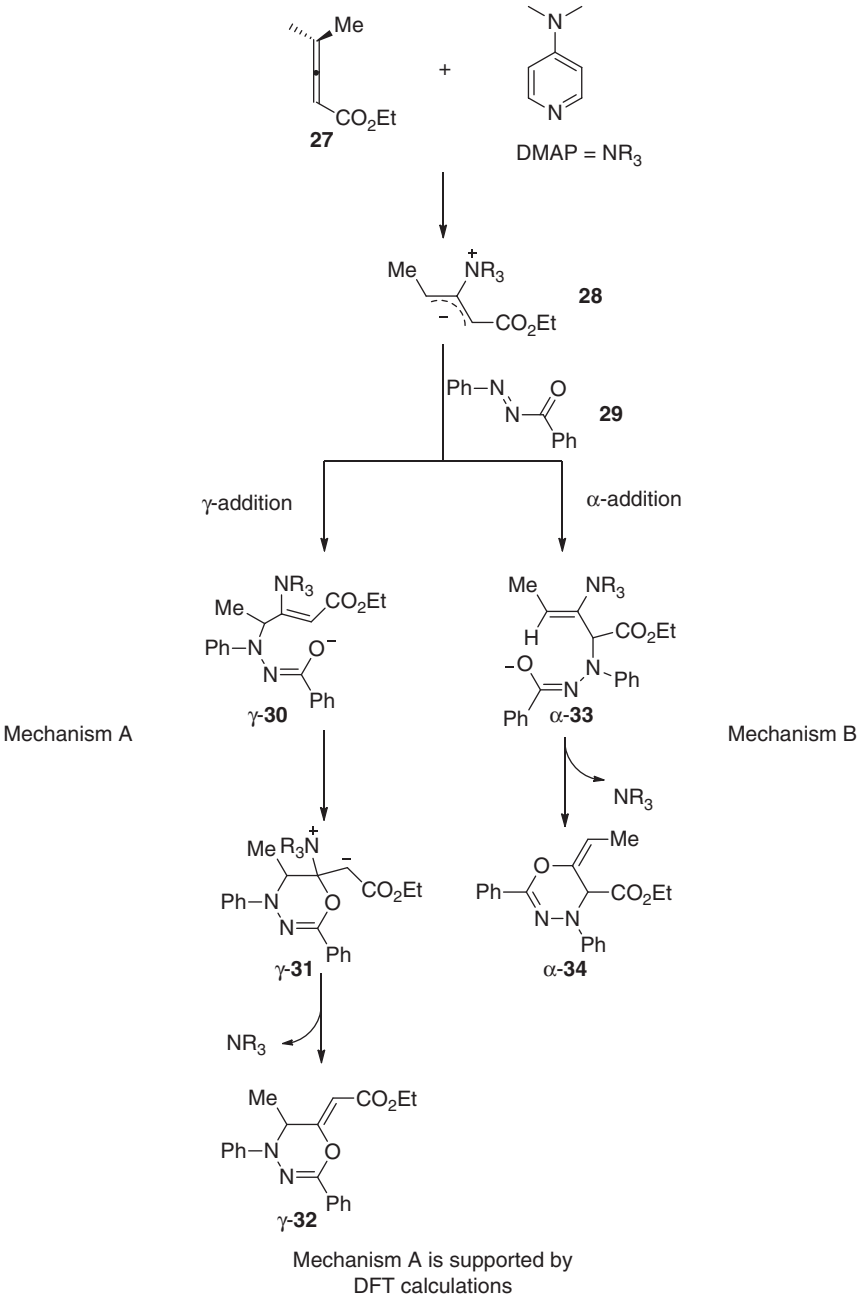

Scheme 1.7 Two possible mechanisms for DMAP-catalyzed [2+4] cycloaddition between γ-methyl allenoate and phenyl(phenyldiazenyl)methanone.

DMAP on **27** to form the zwitterionic intermediate **28**; (ii) γ-addition of **28** to **29** leads to intermediate γ-**30**, (iii) γ-**2** undergoes an intramolecular Michael addition to form the six-membered ring intermediate γ-**31**, and (iv) elimination of catalyst completes the catalytic cycle and yields the final product γ-**32**. The calculated results show that the first step is the rate-determining step. The second step is calculated to be both the regio- and enantio-selectivity-determining step.

Subsequently, investigations were conducted on the mechanisms and stereoselectivities of the [4+2] cycloaddition reaction of methylallenoate with methyleneindolonone **35** catalyzed by DABCO to give product *E*-**36** (Scheme 1.8a) and by DMAP to afford *Z*-**36** as major product (Scheme 1.8b) [15]. The reaction mechanisms were examined with DFT (M06-2X) calculations. Several possible reaction pathways (**paths 1a**, **1b**, and **1c** shown in Scheme 1.9 for DABCO-catalyzed reaction, **paths 2a** and **2b** shown in Scheme 1.10 for DMAP-catalyzed reaction) were located and compared. The results of their studies reveal that for both reactions, three reaction stages are necessary: nucleophilic addition of the catalyst (DABCO or DMAP) to methylallenoate (Stage 1), addition of the other reactant **35** (Stage 2), intramolecular cycloaddition and liberation of the catalyst (DABCO or DMAP) that afforded the final product (Stage 3). For the DABCO-catalyzed cycloaddition, it was predicted that **path 1a** leading to product *E*-**36** is the most energy favorable pathway among the three possible pathways. The energy barrier for carbon–carbon bond formation step is 23.6 kcal mol^{-1}, which is the rate-determining step. With the DMAP catalyst, the suggested that **path 2b** is preferred; thus, the same reaction gave *Z*-**36** as the major product (Scheme 1.10). The barrier for the rate-determining step (addition of R1 to DMAP) is 25.8 kcal mol^{-1}. The calculated results are in agreement with the experimental findings. Moreover, for both reactions, the analysis of global reactivity indexes has been carried out to demonstrate that the catalyst's nucleophilicity plays a key role in their cycloaddition reaction. Their theoretical studies provided a general mechanistic framework for this kind of organoamine-catalyzed cycloaddition reaction, and rationalized the stereoselectities.

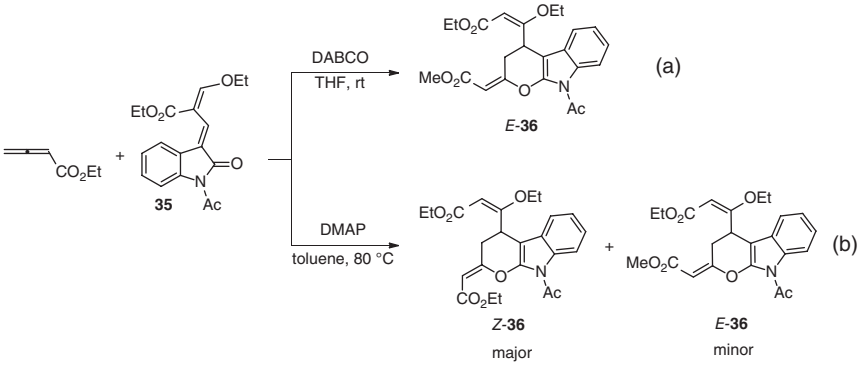

Scheme 1.8 [4+2] cycloaddition reaction of methylallenoate with methyleneindolonone.

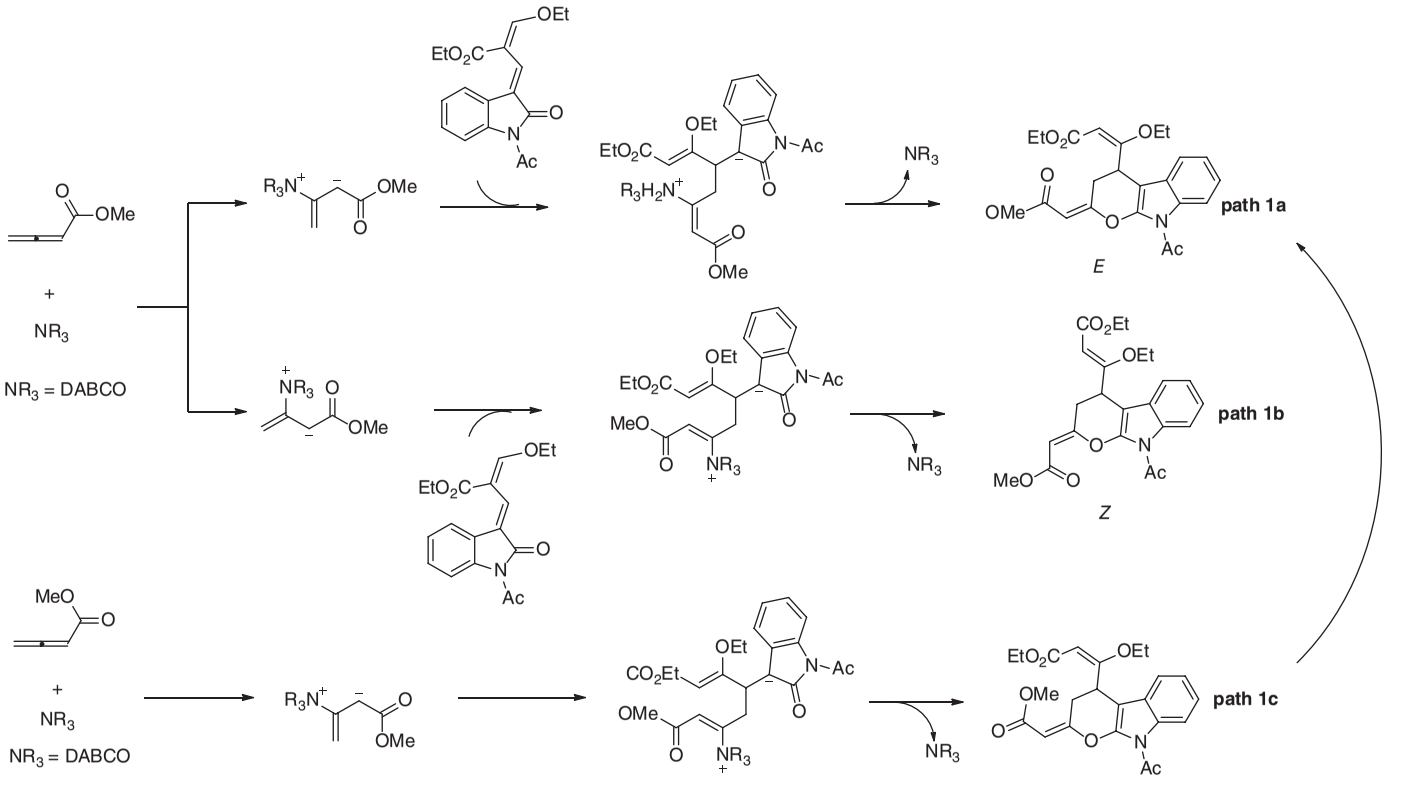

Scheme 1.9 Possible mechanisms for DABCO-catalyzed [4+2] cycloaddition reaction of methylallenoate with methyleneindolonone.

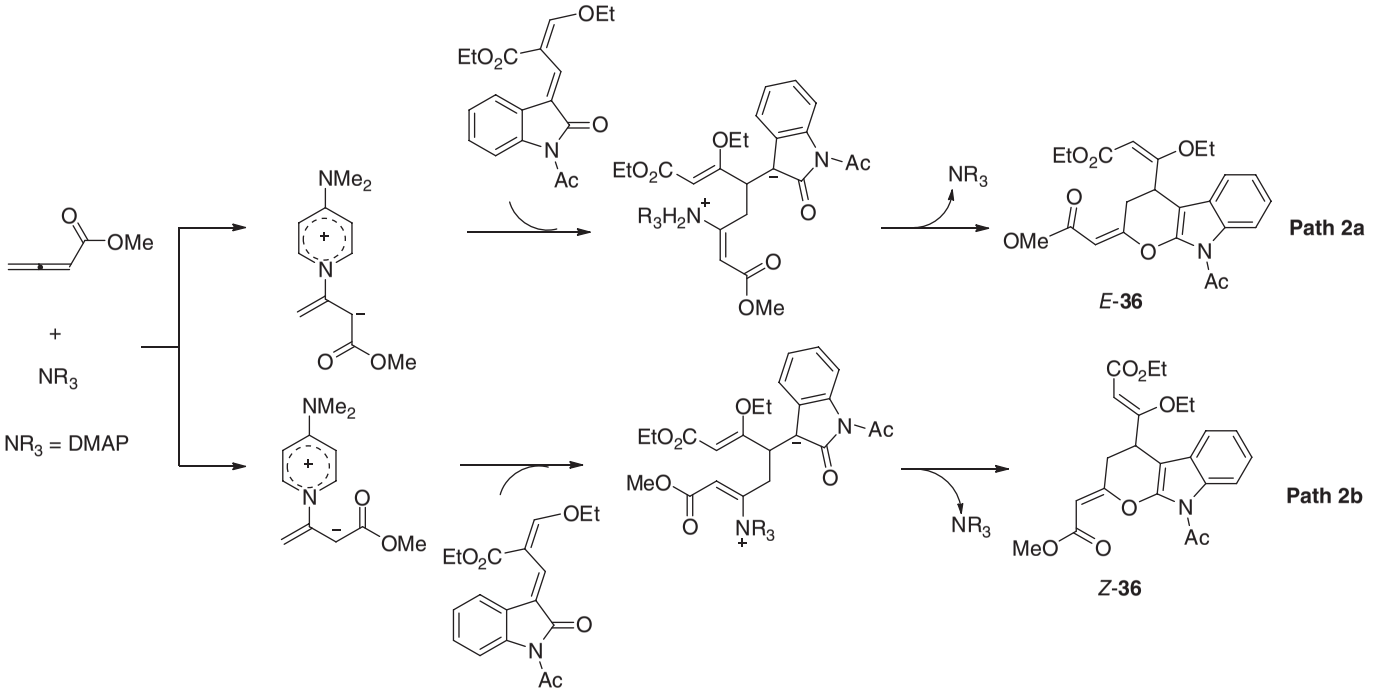

Scheme 1.10 Possible mechanisms for DMAP-catalyzed [4+2] cycloaddition reaction of methylallenoate with methyleneindolonone.

1.2.2 Mechanisms for Common Organophosphine-catalyzed Cycloaddition Reactions

The first seminal report of phosphine-catalyzed [3+2] cycloaddition reaction of allenoate with alkene was published in 1995 by Lu's group [2a]. They initially explored the reaction of ethyl 2,3-butadienoate **37** with methyl acrylate **38** in the presence of triphenylphosphine (50 mol%) in dry benzene at room temperature, and two cycloaddition products **39** and **40** were obtained. In this report, they proposed a plausible mechanism for this reaction as shown in Scheme 1.11. In the proposed mechanism, the zwitterionic inermediate **41** is generated readily through addition of phosphine to the 2,3-butadienoate **37**. The zwitterionic inermediate **41** undergoes a [3+2] cycloaddition with an electron-deficient alkene **38** to give phosphrous ylides **42** and **43**. Then, an intramolecular [1, 2] proton transfer occurs to convert the phosphorus ylides to intermediates **44** and **45**, which, upon elimination of the phosphine catalyst, afford the final cycloadducts **39** and **40**.

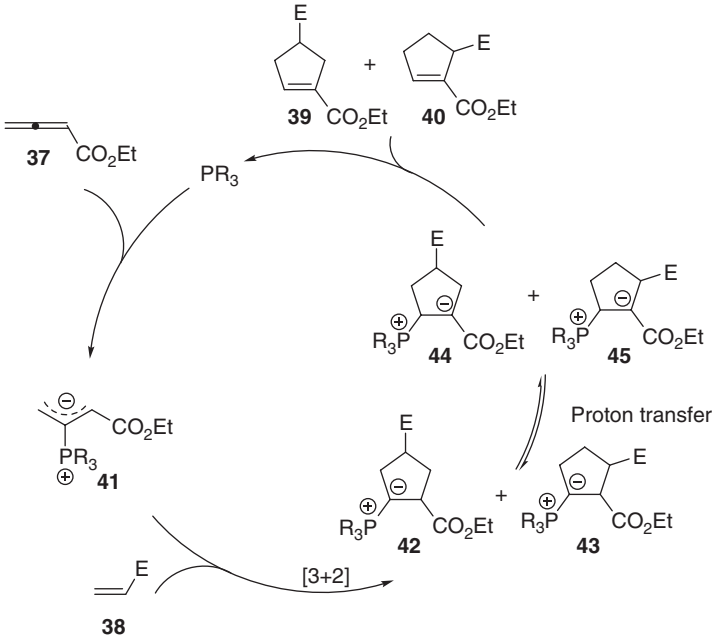

Scheme 1.11 The mechanism of phosphine-catalyzed [3+2] cycloaddition reaction of allenoate with alkene proposed by Lu's group.

Although the mechanism for phosphine-catalyzed [3+2] cycloaddition reaction of allenoate with electron-deficient alkene was first proposed by Lu's group (see Scheme 1.11), the detailed mechanism was not systematically investigated for a long time. In 2007, Yu's group studied the detailed mechanism for this reaction through DFT calculations [16]. Subsequently, Yu's group continued to investigate the detailed mechanism of the phosphine-catalyzed [3+2]

cycloaddition reactions of allenoates and electron-deficient alkenes with the aid of DFT calculations and kinetic experiments [17]. They suggested that this reaction proceeded via the following consecutive steps: (i) *in situ* generation of a 1,3-dipole **46** from nucleophilic addition of phosphine to allenoate; (ii) the first carbon–carbon bond formation to give intermediate **47** and then the second carbon–carbon bond formation occurring to provide [3+2] cycloaddition intermediate **48**, which takes place in a stepwise manner; (iii) association of a water molecule with the intermediate **48** to give a complex **49**, then proton transfer from water to the carbon atom connected with the phosphorus atom occurs to afford a contact ion pair **50**, which undergoes another proton transfer to give complex **51**; (iv) elimination of water to furnish intermediate **52**; and (v) elimination of the phosphine catalyst to afford product **53** (Scheme 1.12). They concluded that the phosphine-catalyzed [3+2] cycloaddition of allenoate with electron-deficient alkene is a stepwise process, and that the generally accepted intramolecular [1, 2] proton shift in the phosphine-catalyzed [3+2] cycloaddition of allenoate with electron-deficient alkene was not possible owing to the very high activation barrier. However, a trace amount of water can assist the [1, 2] proton shift process.

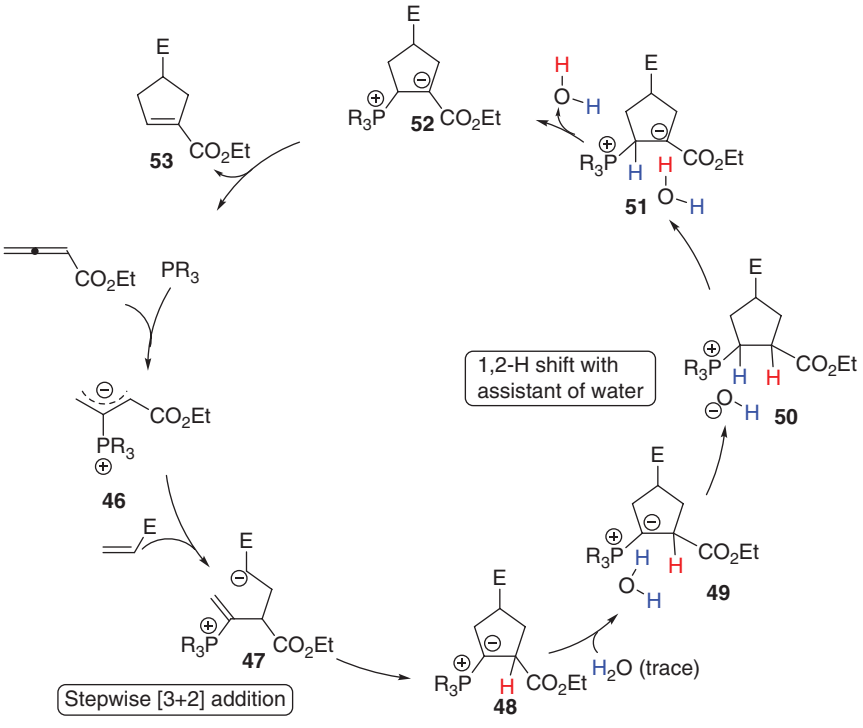

Scheme 1.12 The detailed mechanism for phosphine-catalyzed [3+2] cycloadditions proposed by Yu's group.

Through computational analysis at the B3LYP/6-31G(d) level of theory, Dudding and Kwon almost simultaneously investigated phosphine-catalyzed cycloaddition reactions of acrylates, imines, and aldehydes with allenoates, verified that this phosphine-catalyzed [3+2] cycloaddition reaction proceeded in a stepwise manner, and provided a rational for the reaction regioselectivity [18]. The reaction started from the addition of phosphine to allenoate to generate the zwitterionic intermediate as commonly suggested step in organocatalytic cycloaddition reaction (Scheme 1.13). It was already established that acrylate **54** and imine **55** could undergo predominant α-addition to zwitterionic intermediate **46** to afford [3+2] cycloaddition products (Scheme 1.13, **paths a** and **b**). However, using aldehyde **56** as a substrate, a γ-selective [2+2+2] cycloaddition reaction took place to afford dioxanylidene (*E*)-**57** and (*Z*)-**57** (*E*:*Z* > 8 : 1) with exclusive *cis*-diastereoselectivity (Scheme 1.13, **path c**) [3d]. Through extensive DFT calculations, an excellent level of correlation between the calculated regioselectivities and experimental results was observed. Based on the calculation results, they verified that this phosphine-catalyzed [3+2] cycloaddition reaction proceeded in a stepwise manner, and revealed that Lewis acid activation, strong hydrogen bonding (H-bonding), and minimization of unfavorable

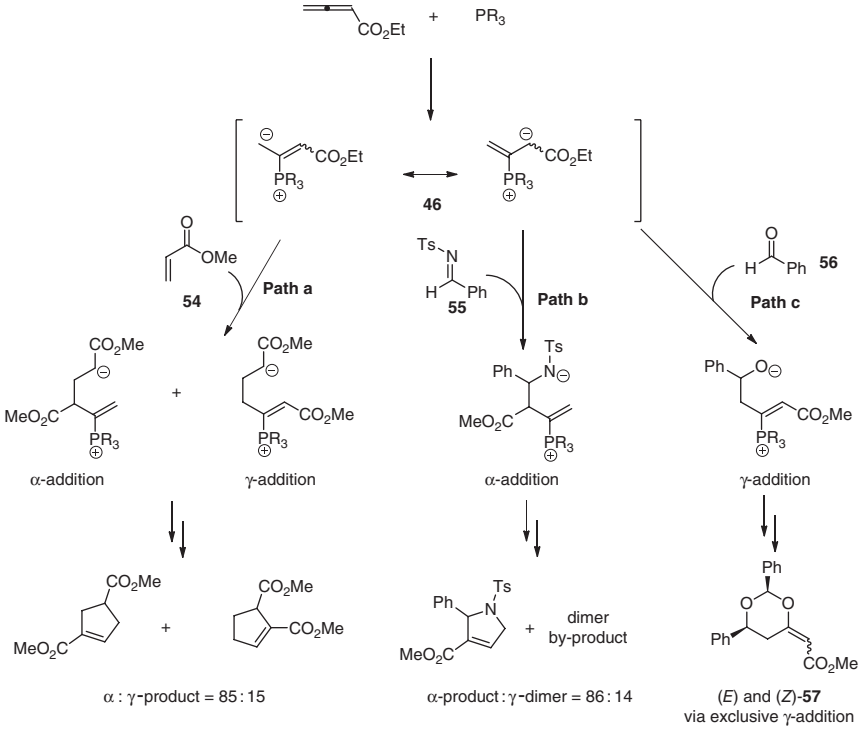

Scheme 1.13 The proposed mechanisms for phosphine-catalyzed cycloaddition reactions of acrylates, imines, and aldehydes with allenoates.

van der Waals contacts were the critical factors that affected the regioselectivity. Subsequently, they also identified the catalytic role of trace water, which played as a proton-shuttle, for proton transfer step[18a], which agreed with Yu's work [16].

In 2015, Shi's group reported regioselectively catalytic asymmetric [3+2] cycloadditions of benzofuranone-derived olefins **58** with allenoate **59** and substituted allenoates **60** in the catalysis of (*R*)-SITCP **63**, affording different functionalized 3-spirocyclopentene benzofuran-2-ones **61** and **62** in good yields with high enantioselectivities under mild condition (Scheme 1.14). In the meantime, they also rationalized the regioselectivity affected by the γ-substituent of allenoate through DFT calculations [19]. The plausible mechanisms for this phosphine-catalyzed [3+2] cycloaddition have been proposed in Scheme 1.15. They proposed that the reaction started from the formation of a zwitterionic intermediate **64** between allenoate (**59** or **60**) and phosphine. Intermediate **64** acts as a 1,3-dipole and undergoes a [3+2] cycloaddition with benzofuranone **58** to give a phosphrous ylide **65** via a γ-addition or **66** via α-addition. For allenoate **59** (R^3 = H), γ-addition is the main pathway. In contrast, allenoate **60** (R^3 = aryl or alkyl group) mainly undergoes α-addition. Then an intramolecular [1, 2] proton transfer is speculated to convert the phosphorus ylide **65** or **66** to another zwitterionic intermediate **67** or **68**, which, upon elimination of the phosphine catalyst, gives rise to the final cycloadduct **61** or **62**. Through DFT calculations, they verified the proposed mechanism, and revealed that the allenoate having

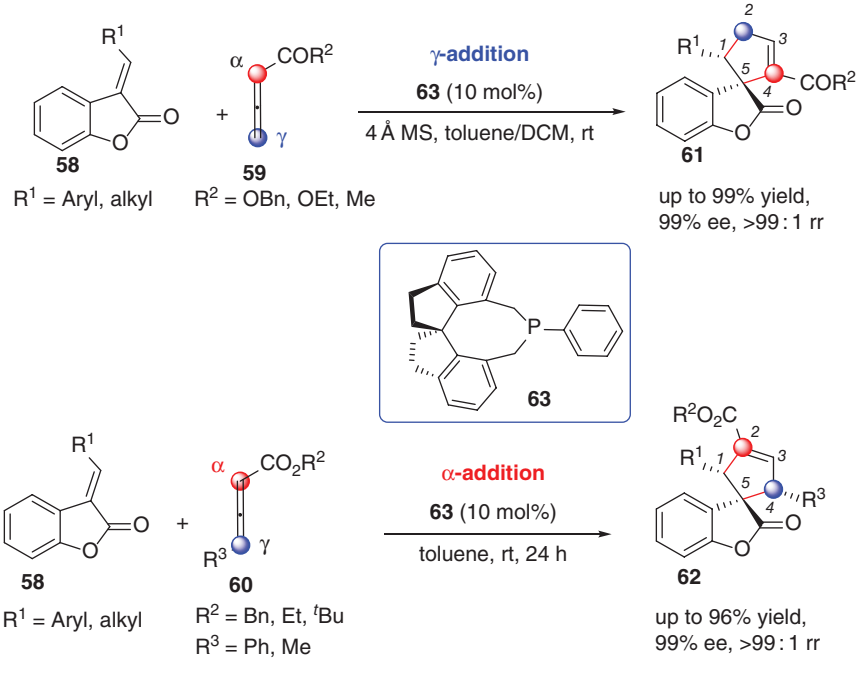

Scheme 1.14 Chiral phosphine-catalyzed tunable cycloaddition reactions of allenoates with benzofuranone derived olefins.

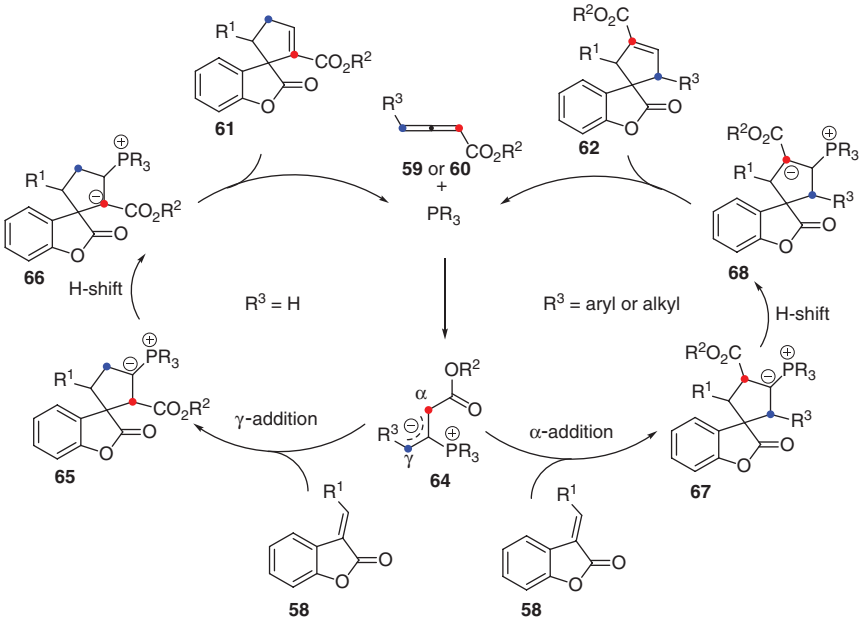

Scheme 1.15 Plausible mechanism for phosphine-catalyzed [3+2] cycloaddition of allenoates with benzofuranone derived olefins.

γ-substituent preferred to undergo α-addition mode due to the steric hindrance between the R^3 substituents and benzofuranone in γ-addition mode.

The idea of employing acetate/*tert*-butylcarbonate-protected β-hydroxymethylacrylates in phosphine catalysis was first introduced by Lu's group in 2003 [20]. By using Morita–Baylis–Hillman alcohol derivatives (MBHAD) as substrates, novel phosphonium species were accessed in the presence of phosphines through new pathways, which subsequently underwent cycloadditions with electron-deficient alkenes to give cycloaddition products. The mechanism proceeds with conjugate addition to the MBHAD **69** with the ejection of the β-leaving group, forming the phosphonium species **70** (Scheme 1.16). The expelled acetate or *tert*-butoxide acts as a base to activate and generate the phosphonium ylide **71**. In the presence of an activated alkene, the following [3+2] cycloaddition reaction occurs to yield a mixture of the cyclopentenes **72** and **73**.

In 2003, the formal [4+2]-cycloadditions of Ts-imines and α-substituted allenoates were first reported by Kwon and co-workers [3a]. They also proposed a plausible mechanism as shown in Scheme 1.17. The [4+2] cycloaddition begins with the initial addition of phosphine to the α-alkyl-2,3-butadienoate **74** to give the phosphonium dienolate **75**. Unlike phosphine-catalyzed [3+2] cycloaddition, addition at the α-position is prohibited by the steric bulkiness; therefore, initial addition occurs only at the γ-position. In the presence of an imine **76**, the zwitterion **77** is subsequently generated. Proton transfer provides the vinyl phosphonium ylide **78**, which is converted to the more stable phosphonium amide

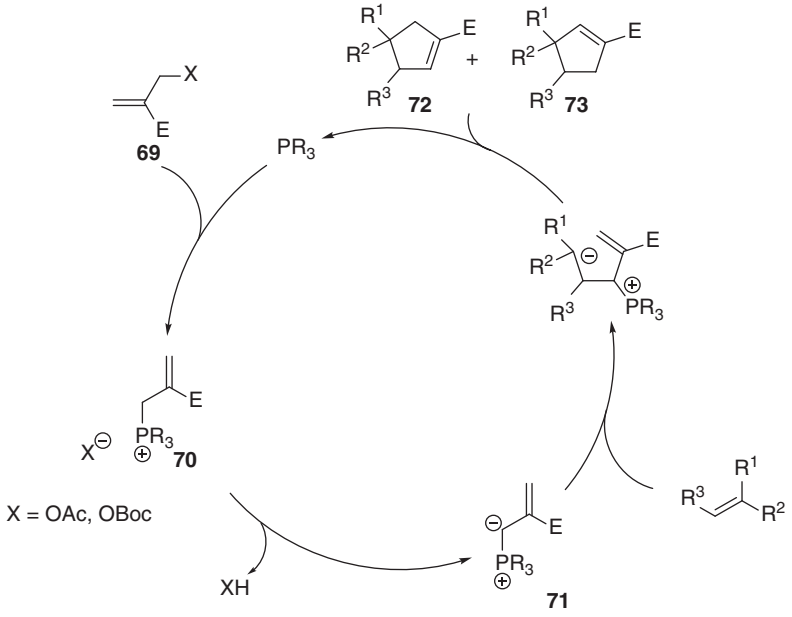

Scheme 1.16 Proposed mechanism for [3+2] cycloaddition of MBHAD and alkene.

zwitterion **79**. The final nitrogen–carbon bond is formed upon the Michael addition of the amide anion, followed by extrusion of the phosphine catalyst to provide the final product tetrahydropyridine **80**.

Although phosphine-catalyzed [4+2] cycloaddition reactions have been developed very well, it is rare to see reports on the studies of the detailed reaction mechanism. In 2012, Han and co-worker investigated phosphine-catalyzed [4+2] cycloadditions between allenoates and electron-poor trifluoromethyl ketones dipolarophiles in continuum solvation using DFT calculations, and the detailed reaction mechanisms as well as the high *cis*-diastereoselectivities of the reactions have been firstly clarified [21]. As illustrated in Scheme 1.18, their calculated results reveal that the whole catalytic process is presumably initiated with the nucleophilic attack of phosphine catalyst at the allenoate to produce the zwitterionic intermediate **81**, which subsequently undergoes γ-addition to the electron-poor C═O of trifluoromethyl ketone to form another intermediate **82**. The following [1,3]-hydrogen shift of **82** is demonstrated to proceed via two consecutive proton transfer steps without the assistance of protic solvent: the anionic O6 of **82** first acts as a base catalyst to abstract a proton from C1 to produce the intermediate **83**, and then the OH group can donate the acidic proton to C3 to complete the [1,3]-hydrogen shift and generate the intermediate **84**. Finally, the intramolecular Michael-type addition generated an intermediate **85,** which released the phosphine catalyst to furnish the final product **86**. High *cis*-diastereoselectivities are also predicted for this reaction, which is in good agreement with the experimental observations. For the reaction of allenoates with trifluoromethyl ketones, the first proton transfer is found to be the

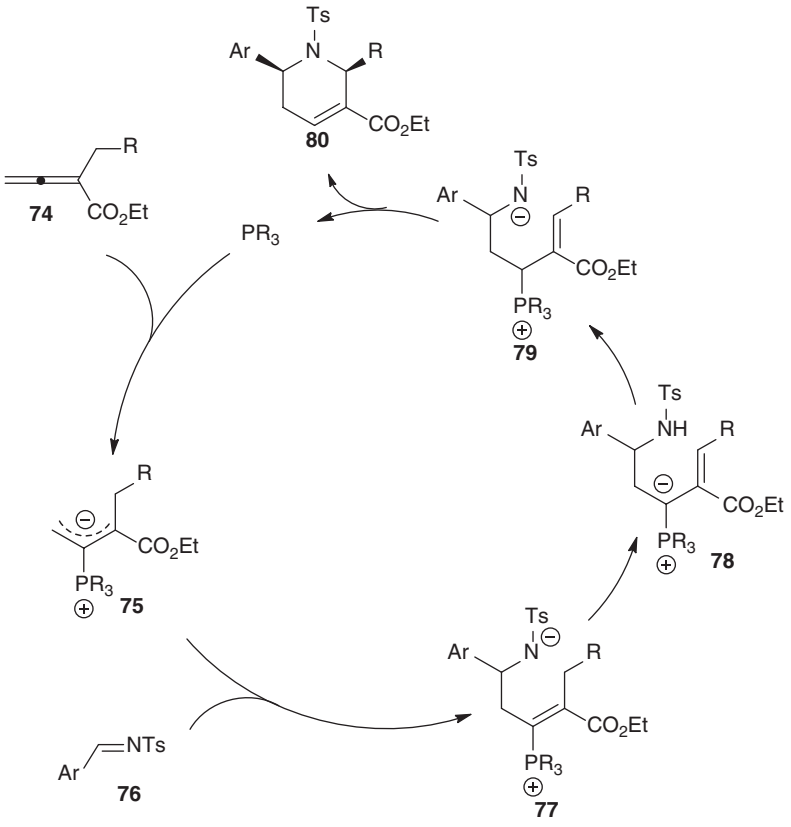

Scheme 1.17 Proposed mechanism for [4+2] cycloaddition reaction of Ts-imine and α-substituted allenoate.

diastereoselectivity-determining step. The cumulative effects of the steric repulsion, electrostatic interaction as well as other weak interactions appear to contribute to the relative energies of transition states leading to the diastereomeric products. In a similar manner, they also investigated the mechanism for the phosphine-catalyzed [4+2] cycloadditions between allenoates and imines. The mechanism for phosphine-catalyzed [4+2] cycloaddition of allenoate and imine is quite similar to the mechanism depicted in Scheme 1.18; however, the Michael-type addition is found to be the diastereoselectivity-determining step.

In 2007, Kwon and co-worker [22] demonstrated that the [4+2] mode can apply to highly electron-deficient olefins to enable the synthesis of cyclohexenes. The Lewis base $P(NMe_2)_3$ (**87**) could catalyze the [4+2] cycloaddition of α-methylallenoate (**88**) and activated alkene (benzylidenemalononitrile **89**) to exclusively afford cyclohexene **90a** [the ratio of **90a**/**90b** being 100 : 0] (Scheme 1.19). Wang and co-workers conducted DFT calculations to understand the [4+2] cycloaddition reaction between α-methylallenoate (**88**) and benzylidenemalononitrile (**89**) catalyzed by $P(NMe_2)_3$ (**87**) [23]. The cyclohexene **90a** was identified as the predominated product in the experiment. Based

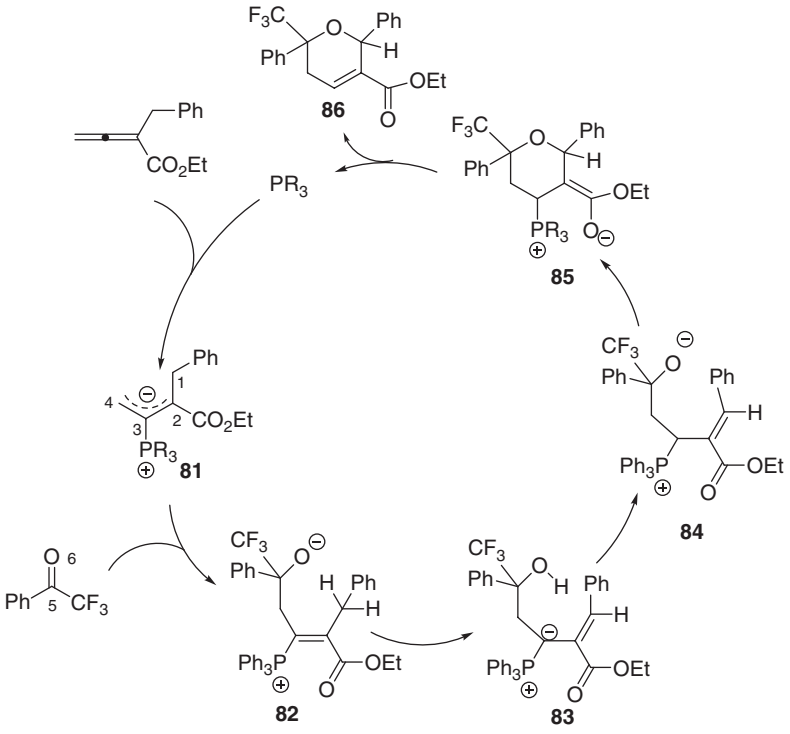

Scheme 1.18 A plausible mechanism for phosphine-catalyzed [4+2] cycloaddition of allenoate and trifluoromethyl ketone.

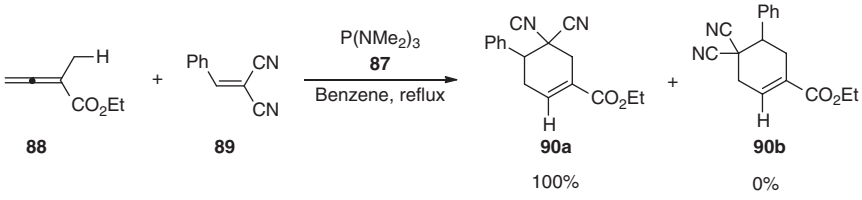

Scheme 1.19 The [4+2] cycloaddition reaction of α-methylallenoate and benzylidenemalononitrile catalyzed by $P(NMe_2)_3$.

on the DFT calculation results, they verified the proposed mechanism and accounted for the exclusive regioselectivity. Their studies show that the catalytic cycle of the reaction can be characterized similarly by three stages (Scheme 1.20): Stage 1 being the addition of catalyst **87** to allenoate **88**, generating the 1,3-dipole intermediate **91**; Stage 2 being the addition of alkene **89** to **91** to give intermediate **92**, followed by hydrogen transfer to generate the allylic phosphonium intermediate **93** and ring closure in **93** to give the six-membered-ring intermediate **94**; and Stage 3 being the release of catalyst **87** from **94** to form product **90a**. Their calculation results reveal that the pathway leading to

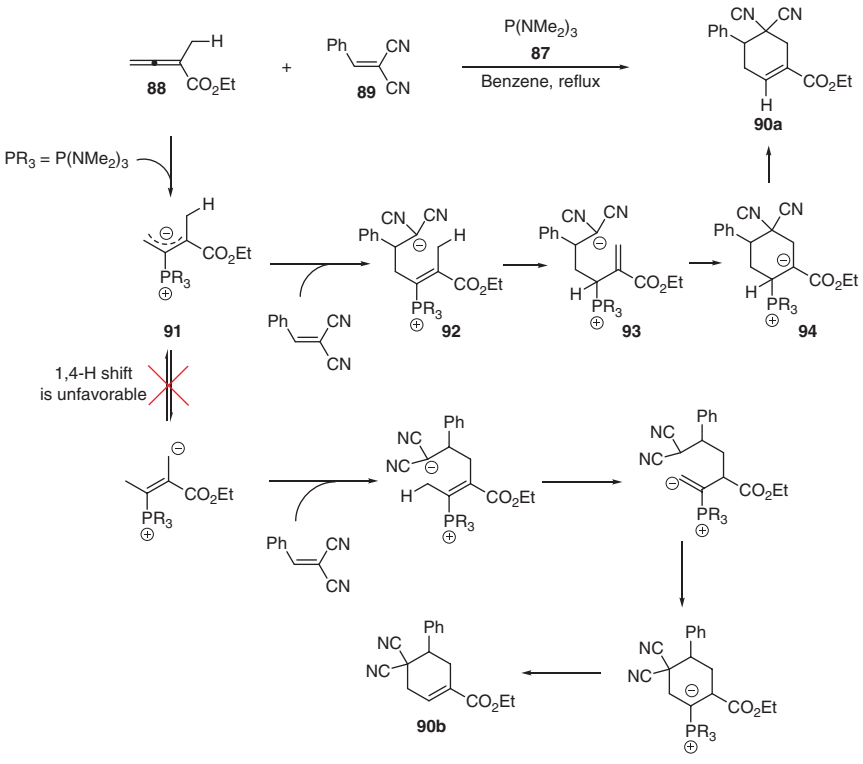

Scheme 1.20 A plausible mechanism for [4+2] cycloaddition reaction of α-methylallenoate and benzylidenemalononitrile catalyzed by $P(NMe_2)_3$.

the product **90b** is substantially less favorable due to the difficult 1,4-H shift in this case, which accounts for the exclusive regioselectivity (**90a**/**90b** = 100 : 0) of the reaction. The [4+2] cycloadditions are different from the conventional [3+2] cycloadditions of allenoates and activated alkenes. In the phosphine-catalyzed [3+2] cycloadditions of allenoates and activated alkenes, a trace amount of water was demonstrated to be critical [16], even though the reactions are carried out in so-called "anhydrous" solvents, because water is the only available hydrogen transfer mediator. In other words, the traditional [3+2] cycloadditions would not occur if the solvent was absolutely free of water. In contrast, this [4+2] cycloaddition can take place, even though water is completely absent, because the carbon (C^{CN} of alkene **89**) bearing the nitrile groups can serve as the hydrogen transfer mediator.

1.2.3 Cycloaddition Reaction Modes Influenced By Catalysts

Although the amines and phosphines have some similarity as Lewis base catalysts, they still demonstrate different catalytic properties in some cycloaddition reactions. In the catalysis of phosphine, the [3+2] cycloaddition reactions of allenoates and activated alkenes took place easily; however, switching to amines

as catalysts, the [2+4] cycloaddition reactions or via an intermediate Rauhut–Currier reaction to access [2+4] cycloaddition product occurred. Yu's group investigated the cycloaddition reaction modes affected by catalysts through DFT calculations [24]. The addition of the catalyst to the allenoate is the first step in both pathways followed by the reaction with the enone. Their calculation results reveal that formation of the [3+2] phosphorus ylide is exergonic, and hence, the [3+2] cycloaddition is kinetically favored over the [2+4] addition (Scheme 1.21). Amines do not stabilize [3+2] ammonium ylides; however, electron-withdrawing groups on the enone enable [2+4] cycloadditions (Scheme 1.21). The strength of the electron-withdrawing group further controls the α/γ regioselectivity of the [2+4] cycloaddition, and the analysis of the highest occupied molecular orbital–lowest unoccupied molecular orbital (HOMO–LUMO) interactions explains why only *E*-dihydropyrans from the direct γ-[2+4] cycloaddition have been observed in experiments. The quantum calculations further reveal a new path to the α-[2+4] product starting with an intermediate Rauhut–Currier reaction. This new path is kinetically favored over the direct amine-catalyzed α-[2+4] cycloaddition. Their study explains the origin of different reactivity between phosphine and amine catalysts and the substituent effect of the enone in amine catalysis.

Subsequently, Yu's group further investigated the cycloaddition reactions of allenoates with enones catalyzed by different LB such as phosphines, amines, and NHCs; and they revealed the different catalytic properties of these LB catalysts [25]. Based on their DFT calculations, the addition of LBs to methyl allenoate can yield either *Z*- or *E*-adducts, and the Z-pathway is preferred due to the strong binding electrostatic interactions between the carbonyl oxygen atom and the LB (Scheme 1.22). Among their studied LBs, the formation of NHC·allenoates is the most exergonic. As the dielectric constant of the solvent increases, the stability of the *E*-adducts increases more pronouncedly than that of the *Z*-adducts. The calculated barriers for the S_N2 reaction of the LB·allenoates with CH_3Cl show that Cα in the LB·allenoate is more nucleophilic than Cγ. The adducts can also react with ethylene to form [3+2] ylides. The analysis of the LB-ylides shows that amines form less stable ylides than phosphines, which again are less stable than those derived from NHCs. The ELF analysis reveals a direct correlation between the strength of the ylidic bond and the overall stability of the forming five-membered rings. The LB catalyzed reaction of allenoates with enones can either yield [3+2]-(cyclopentenes) or [2+4]-cycloadducts (dihydropyrans). When phosphines are used as catalysts, the [3+2] cycloaddition dominates, because the ring-closing step is more favorable due to the exergonic formation of P-ylides. The [3+2]-cyclopentene products are also more stable than the [2+4]-dihydropyrans. In general, the [3+2] cycloaddition dominates both kinetically and thermodynamically when phosphines are used as catalysts. If amines are used as catalysts, kinetic control favors the formation of [2+4]-dihydropyrans over the cyclopentenes due to the instability of the [3+2] N-ylides. The LB-catalyzed reaction of allenoates with ketones yields [2+2]-(oxetanes), [3+2]-(dihydrofurans) or [2+2+2]-cycloadducts (1,3-dioxanes). The formation of NHC·allenoates is extremely exergonic and these adducts are even more stable than the expected [2+2]-products. Hence, the thermodynamically controlled [2+2+2] annulation is favored with NHCs as catalysts. On the other hand, the

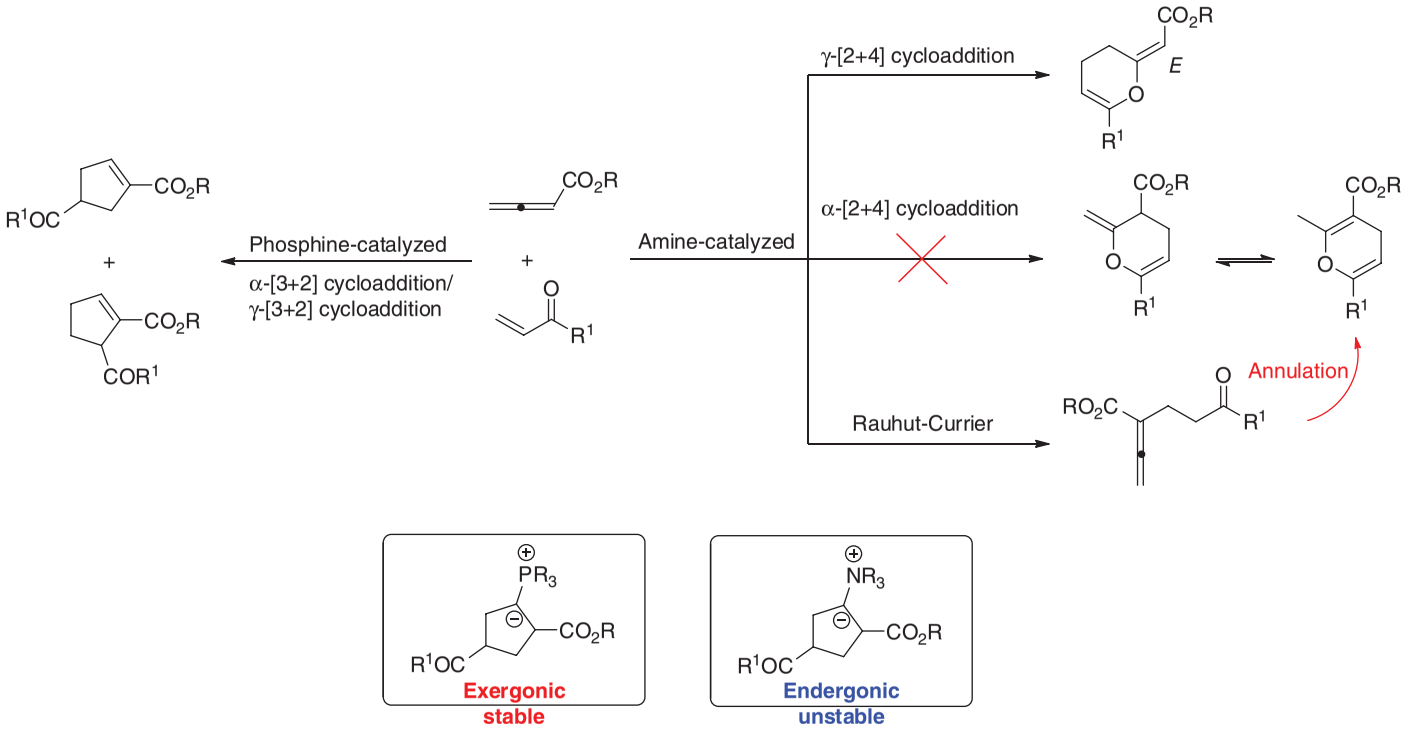

Scheme 1.21 The origin of different reactivity between phosphine and amine catalysts.

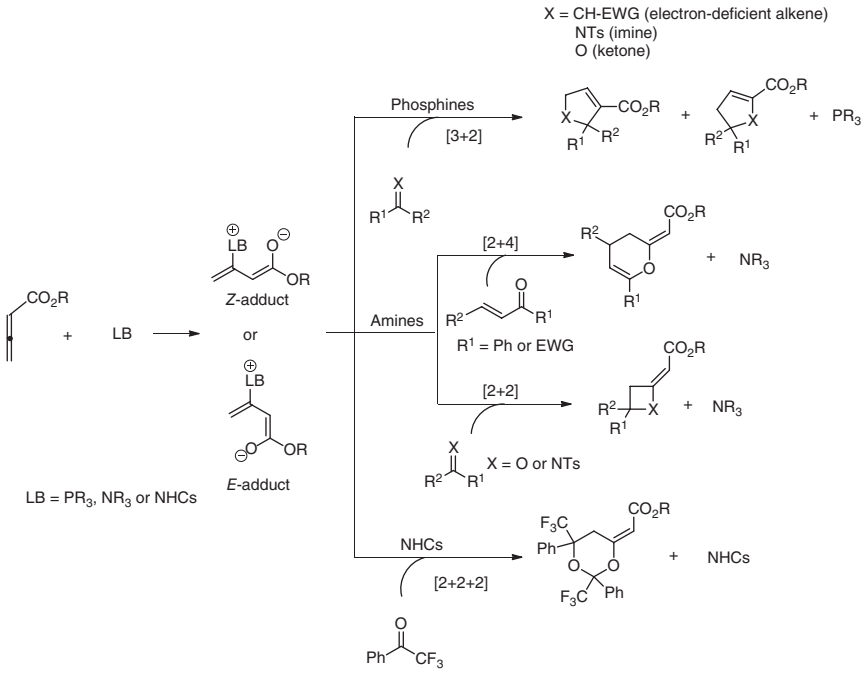

Scheme 1.22 The cycloaddition reaction modes affected by different LB catalysts.

formation of DABCO·allenoates is endergonic, which leads to the kinetically preferred [2+2] products. When PPh_3 is used as the catalyst, the [3+2] cycloaddition is both thermodynamically and kinetically favored. Despite NHCs having high initial reactivity, NHCs are less efficient than phosphines and N-based LBs because the NHC·allenoate intermediates are extremely stable.

References

1 (a) Kirsch, S.F. (2006). *Org. Biomol. Chem.* **4**: 2076–2080.
(b) Hou, X.-L., Yang, Z., Yeung, K.-S., and Wong, H.N.C. (2008). *Progress in Heterocyclic Chemistry*, vol. **19**. Pergamon: Oxford.
(c) Katritzky, A.R., Ramsden, C.A., Scriven, E.F.V., and Taylor, R.J.K. (2008). *Comprehensive Heterocyclic Chemistry III*. Oxford: Elsevier.

2 (a) Zhang, C. and Lu, X. (1995). *J. Org. Chem.* **60**: 2906–2908.
(b) Xu, Z. and Lu, X. (1998). *J. Org. Chem.* **63**: 5031–5041.
(c) Du, Y. and Lu, X. (2003). *J. Org. Chem.* **68**: 6463–6465.

3 (a) Zhu, X.-F., Lan, J., and Kwon, O. (2003). *J. Am. Chem. Soc.* **127**: 4716–4717.
(b) Tran, Y.S. and Kwon, O. (2005). *Org. Lett.* **7**: 4289–4291.
(c) Zhu, X.-F., Schaffner, A.-P., Li, R.C., and Kwon, O. (2005). *Org. Lett.* **7**: 2977–2980.
(d) Zhu, X.-F., Henry, C.E., Wang, J. et al. (2005). *Org. Lett.* **7**: 1387–1390.
(e) Guo, H., Xu, Q., and Kwon, O. (2009). *J. Am. Chem. Soc.* **131**: 6318.

(f) Creech, G.S., Zhu, X.F., Fonovic, B. et al. (2008). *Tetrahedron* **64**: 6935–6942.
(g) Creech, G.S. and Kwon, O. (2008). *Org. Lett.* **10**: 429–432.
(h) Henry, C.E. and Kwon, O. (2007). *Org. Lett.* **9**: 3069–3072.
(i) Cai, L., Zhang, K., and Kwon, O. (2016). *J. Am. Chem. Soc.* **138**: 3298–3301.
(j) Villa, R.A., Xu, Q., and Kwon, O. (2012). *Org. Lett.* **14**: 4634–4637.
(k) Barcan, G.A., Patel, A., Houk, K.N., and Kwon, O. (2012). *Org. Lett.* **14**: 5388–5391.
(l) Andrews, I.P. and Kwon, O. (2012). *Chem. Sci.* **3**: 2510–2514.
(m) Guo, H., Xu, Q., and Kwon, O. (2009). *J. Am. Chem. Soc.* **131**: 6318–6319.

4 (a) Zhao, G.L. and Shi, M. (2005). *J. Org. Chem.* **70**: 9975–9984.
(b) Guan, X.Y. and Shi, M. (2009). *J. Org. Chem.* **74**: 1977–1981.
(c) Lian, Z. and Shi, M. (2012). *Eur. J. Org. Chem.* **2012**: 581–586.
(d) Lian, Z. and Shi, M. (2012). *Org. Biomol. Chem.* **10**: 8048–8050.
(e) Hu, F., Wei, Y., and Shi, M. (2012). *Tetrahedron* **68**: 7911–7919.
(f) Deng, H.P., Wang, D., Wei, Y., and Shi, M. (2012). *Beilstein J. Org. Chem.* **8**: 1098–1104.
(g) Zhang, X.C., Cao, S.H., Wei, Y., and Shi, M. (2011). *Chem. Commun.* **47**: 1548–1550.
(h) Xing, J., Lei, Y., Gao, Y.N., and Shi, M. (2017). *Org. Lett.* **19**: 2382–2385.
(i) Gao, Y.-N., Xu, Q., Wei, Y., and Shi, M. (2017). *Adv. Synth. Catal.* **359**: 1663–1671.
(j) Wang, D., Lei, Y., Wei, Y., and Shi, M. (2014). *Chem. Eur. J.* **20**: 15325–15329.

5 (a) Wang, H., Zhou, W., Tao, M. et al. (2017). *Org. Lett.* **19**: 1710–1713.
(b) Li, Y., Su, X., Zhou, W. et al. (2015). *Chem. Eur. J.* **21**: 4224–4228.

6 (a) Wang, C., Jia, H., Zhang, C. et al. (2017). *J. Org. Chem.* **82**: 633–641.
(b) Yuan, C., Zhou, L., Xia, M. et al. (2016). *Org. Lett.* **18**: 5644–5647.
(c) Wang, C., Gao, Z., Zhou, L. et al. (2016). *Org. Lett.* **18**: 3418–3421.
(d) Li, Z., Yu, H., Liu, Y. et al. (2016). *Adv. Synth. Catal.* **358**: 1880–1885.
(e) Gao, Z., Wang, C., Yuan, C. et al. (2015). *Chem. Commun.* **51**: 12653–12656.

7 (a) Liang, L. and Huang, Y. (2016). *Org. Lett.* **18**: 2604–2607.
(b) Li, E., Jin, H., Jia, P. et al. (2016). *Angew. Chem. Int. Ed.* **55**: 11591–11594.
(c) Li, E., Jia, P., Liang, L., and Huang, Y. (2014). *ACS Catal.* **4**: 600–603.

8 (a) Ni, C., Zhou, W., and Tong, X. (2017). *Tetrahedron* **73**: 3347–3354.
(b) Gu, Y., Hu, P., Ni, C., and Tong, X. (2015). *J. Am. Chem. Soc.* **137**: 6400–6406.

9 (a) Wei, Y. and Shi, M. (2014). *Chem. Asian J.* **9**: 2720–2734.
(b) Fan, Y.C. and Kwon, O. (2013). *Chem. Commun.* **49**: 11588–11619.
(c) Zhao, Q.Y., Lian, Z., Wei, Y., and Shi, M. (2012). *Chem. Commun.* **48**: 1724–1732.
(d) Ye, L.W., Zhou, J., and Tang, Y. (2008). *Chem. Soc. Rev.* **37**: 1140–1152.

10 (a) Wynberg, H. and Staring, E.G.J. (1985). *J. Org. Chem.* **50**: 1977–1979.
(b) Wynberg, H. and Staring, E.G.J. (1982). *J. Am. Chem. Soc.* **104**: 166–167.

11 Dijkstra, G.D.H., Kellogg, R.M., Wynberg, H. et al. (1989). *J. Am. Chem. Soc.* **111**: 8069.

12 Zhao, G.-L., Huang, J.-W., and Shi, M. (2003). *Org. Lett.* **5**: 4737–4739.

13 Yang, H.B., Yuan, Y.C., Wei, Y., and Shi, M. (2015). *Chem. Commun.* **51**: 6430–6433.

14 Li, Y. and Du, S. (2016). *RSC Adv.* **6**: 84177–84186.

15 Li, Y., Liu, T., and Fu, W. (2017). *Int. J. Quantum Chem.* **117**: e25408.
16 Xia, Y., Liang, Y., Chen, Y. et al. (2007). *J. Am. Chem. Soc.* **129**: 3470–3471.
17 (a) Liang, Y., Liu, S., Xia, Y. et al. (2008). *Chem. Eur. J.* **14**: 4361–4373.
(b) Liang, Y., Liu, S., and Yu, Z.-X. (2009). *Synlett* 905.
18 (a) Mercier, E., Fonovic, B., Henry, C. et al. (2007). *Tetrahedron Lett.* **48**: 3617–3620.
(b) Dudding, T., Kwon, O., and Mercier, E. (2006). *Org. Lett.* **8**: 3643–3646.
19 Wang, D., Wang, G.-P., Sun, Y.-L. et al. (2015). *Chem. Sci.* **6**: 7319–7325.
20 Du, Y., Lu, X., and Zhang, C. (2003). *Angew. Chem. Int. Ed.* **42**: 1035–1037.
21 Qiao, Y. and Han, K.L. (2012). *Org. Biomol. Chem.* **10**: 7689–7706.
22 Tran, Y.S. and Kwon, O. (2007). *J. Am. Chem. Soc.* **129**: 12632–12633.
23 Zhao, L., Wen, M., and Wang, Z.-X. (2012). *Eur. J. Org. Chem.* **2012**: 3587–3597.
24 Huang, G.T., Lankau, T., and Yu, C.H. (2014). *J. Org. Chem.* **79**: 1700–1711.
25 Huang, G.T., Lankau, T., and Yu, C.H. (2014). *Org. Biomol. Chem.* **12**: 7297–7309.